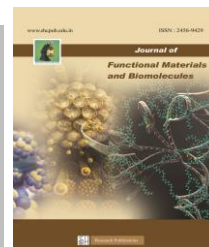




SACRED HEART RESEARCH PUBLICATIONS

Journal of Functional Materials and Biomolecules

Journal homepage: www.shcpub.edu.in



ISSN: 2456-9429

A study on Polyoxometalate doped Natural polymers

Jothi Selvam¹, Bharath Samannan¹, Praveen Peter¹, Jeyabalan Thavasikani^{1*}

Received on 12 December 2019, accepted on 15 December 2019,

Published online on 26 December 2019

Abstract

Polyoxometalates (POMs) have demonstrated strong potential in various fields, such as catalysis, magnetism, medicine, photochemistry and materials science, for their remarkable physical and chemical properties. The aim of this study is to analyze chemical, physical and morphological properties of Mn-based polyoxometalate doped natural polymers (*Prosopis juliflora* resin). The Mn-based polyoxometalate (Mn-POM) doped polymers has been synthesized and characterized through various spectroscopic techniques like FT-IR spectra, which shows the presence of functional groups and SEM morphology shows morphological structure. XRD results give crystalline grain size. The antibacterial activity is also studied.

Keywords: Polyoxometalates, Polyacid, Natural polymer resin.

1 Introduction

Polyoxometalates (POMs) are an exceptional family of inorganic clusters consisting of Mo, V, W, etc [1-4]. Since the first POMs, $(\text{NH}_4)_3[\text{PMo}_{12}\text{O}_{40}]$ (PMo_{12}), reported by Berzelius in 1826, the POMs chemistry, a special branch of coordination chemistry, has aroused wide attention with the development of structure characterization technology [5]. Polyoxometalates are often utilized as well-defined models to study selective oxidation and acid catalysis by metal oxide [6]. Keggin type POMs ($\text{XM}_{12}\text{O}_{40}$) act as oxidation and acid catalysts, and by varying the heteroatom ($X = \text{P}^{5+}$, Si^{4+} and As^{5+}) and framework metal atoms ($M = \text{Mo}^{6+}$, V^{5+} or W^{6+}), one may vary the acid and redox properties systematically while maintaining the same framework structure [7, 8].

POM science is no longer focused specially on the design and synthesis of novel structures but is trending toward the consideration of more interdisciplinary multifunctional materials and related fields to diversify the future possibilities of POMs [9, 10]. As could be expected, the intrinsic topology structures of POMs shown in Fig.1. POMs are broadly applicable include in optics, electrochemistry, magnetism, medicine, and catalysis [11-13].

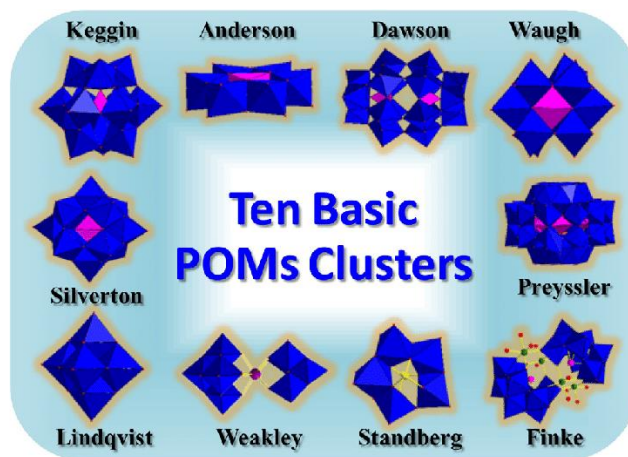


Fig.1. Ten basic structural topology of POMs clusters

The PA is the metal oxygen clusters with MO_6 units set to bridge the oxygen atoms. PA is early transition metal which is used mostly in the different fields. Polyacid is one of the most interesting areas in Inorganic chemistry, exhibiting at various promising properties and applications. Polyacid have a molecular weight as well as temperature response over doped polymer material [14]. Polyacid (PA) is shown as an effective study in last decades of geometric and electronic structural property. Polyacid doped natural polymers which have three major challenges in ions pairing, selectivity, stability, and reactivity [15-16].

Polyacid (PA) is a sub-division of MO (metal oxide) with specific, unique physical and chemical properties, as well as prospective applications like structural materials, medicines, catalysts. Polyacid doped Natural polymer give an important studies, such as *Prosopis juliflora* Resin in Figs.2 and 3. Therefore, it is found that the Polyacid doped natural polymer exhibit the high catalytic activity to a new properties and applications [17]. In this paper, a study on Polyoxometalate doped natural polymer has been discussed.

* Corresponding author: e-mail jayabalandr@gmail.com, Department of Chemistry, Sacred Heart College, Tirupattur-635 601, Tamil Nadu, India.



Fig.2. Prosopis juliflora



Fig.3. Prosopis juliflora resin

2 Experimental

2.1. Chemicals and Reagents

All reagents used in the experiments were of analytical grade. Ammonium molybdate, Manganese (II) sulphate, Disodium hydrogen phosphate, Potassium persulphate, concentrated Nitric acid from Merck.

2.2. Synthesis of PA doped Natural polymer

The complex is prepared by mixing of ammonium molybdate solution (4 g, 10 ml) with the solution of disodium hydrogen phosphate (1 g, 10 ml) followed by the addition of few drops of nitric acid. To this mixture (1 g of Resin, 10 ml) resin solution is added continuously with stirring. The formed products are filtered and dried.

2.3. Synthesis of MnPA doped Natural polymer

The complex is prepared by adding 1 g of manganese (II) sulphate and the oxidant, potassium persulphate in 10 ml of distilled water. To this content, the solution of ammonium molybdate (4 g, 10 ml) is added. To this acidified solution, 1 g of disodium hydrogen phosphate is added with continuous stirring and heated. To the prepared Mn-PA solution, Natural Polymer (R) is added with continuous stirring. The formed products are filtered and dried.

2.4. Analytical measurements

The sample was analyzed using various analytical techniques. IR spectrum was recorded using Perkin Elmer spectrometer (PES) was recorded in the spectral range of 4000-400 cm^{-1} . The morphology of the doped was investigated using scanning electron microscope (JASCO JSM 6390 SEM). The XRD spectrum was recorded using (SHIMAZDU XRD-6000) diffraction analysis.

3 Results and Discussion

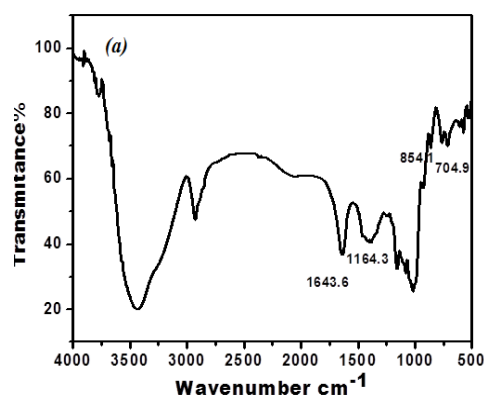
3.1. FTIR spectra

The FT-IR spectra of PA, MnPA, PA-R and MnPA-R are shown in Fig.4. The IR spectral data of PA, MnPA, PA-R and MnPA-R are given in Table.1. The tentative band assignment is based on the literature[18].

In Fig. 4a and 4c PA exhibit intensive three characteristic peaks at 1643 cm^{-1} is assigned to intra ring (C=C) vibration. The peak at 1067 cm^{-1} indicates the absorption of P-O stretching vibration. The peak at 974 cm^{-1} is assigned to Mo-Ot stretching. A peak at 854 cm^{-1} is stretching frequency of M-O-M bonds. The stretching vibrations of M-O-X is at 704 cm^{-1} (X=P). These sharp peak splits indicates that the PA structure was maintained after immobilization.

In Fig.4b the peak at 786 cm^{-1} indicates the stretching frequency of M-O-X (X=Mn). The tentative assignment of PA doped natural polymers are 1063 cm^{-1} P-O; 965 cm^{-1} Mo-Ob; 787 cm^{-1} , polymers like Prosopis juliflora resin (R), assignments based on the one at 964 cm^{-1} split into three spectral peaks which indicate the presence of Mn in the PA lattice (Mn-PA) as shown in Fig.4d.

Fig.4c shows PA doped natural polymers (Resin) in which peaks at 1062 cm^{-1} is stretching frequency P-O. This vibrating peak revealed that the PA doped natural polymers; structure is remaining intact after doping.



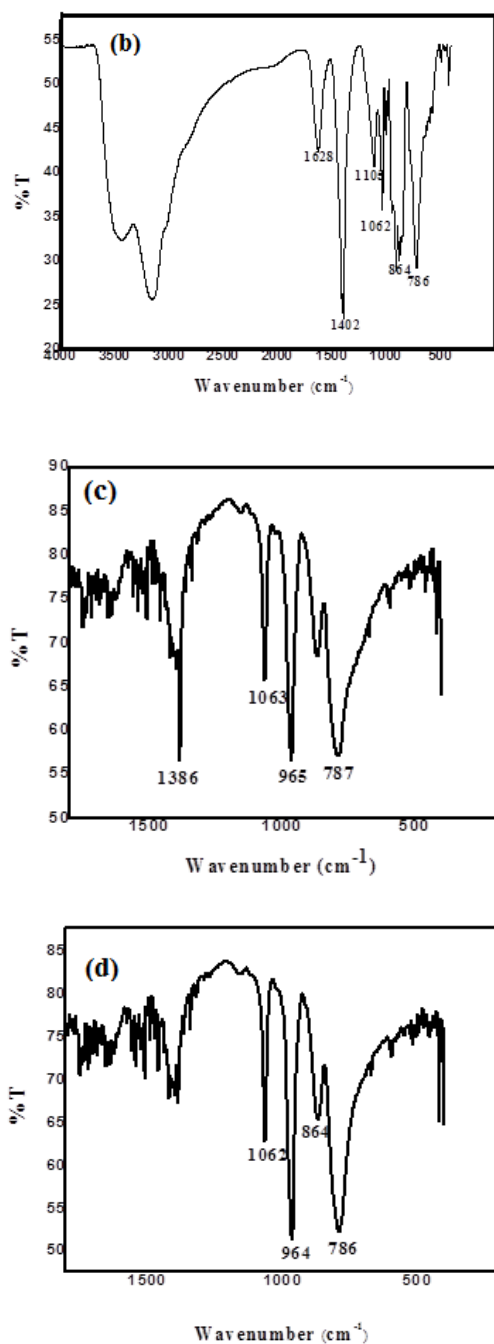


Fig.4. IR spectra of (a) PA, (b) MnPA, (c) PA-R and (d) MnPA-R

Table1: IR spectral data of PA, MnPA, PA-R and MnPA-R

Compounds	P-O (cm^{-1})	Mo-Ot (cm^{-1})	M-O-M (cm^{-1})	M-O-X (X=P&Mn) (cm^{-1})
PA	1067	974	854	704
MnPA	1055	969	865	786
PA-R	1063	965	866	787
MnPA-R	1062	964	864	786

3.2. Scanning electron microscopic studies (SEM)

The SEM morphology of Fig. 5a and 5b show that uniform formation of granules is around 5mm. The PA and MnPA doped natural polymers (*Prosopis juliflora* resin) synthesized under the same conditions, respectively. Fig. 5c and 5d show that the spherical structure of the sample with the average diameter of 5 mm. Thus, the formed SEM morphology shows that the structure of PA and Mn-PA in intact in doped natural polymers [19]. The SEM images which are confirm that the polyacid is loaded over the natural polymer (resin) material. The formation of host-guest compound is confirmed by SEM images.

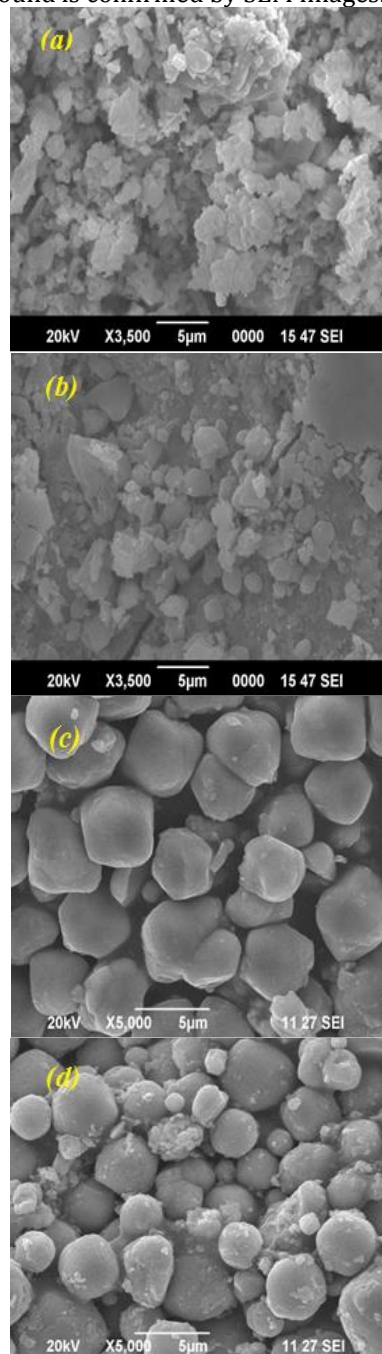


Fig.5. SEM morphology of (a) PA (b) MnPA (c) PA-R and (d) MnPA-R

3.3. X-Ray Diffractions (XRD)

The XRD pattern of PA are shown Fig.6a contains some sharps peaks at 11.19°, 15.45°, and 27.59°, representing the crystal planes of (200), (100), (111), of PA respectively. In Fig.6b shows XRD pattern of MnPA contains some sharps peaks at 28.50°, 30.27°, and 41.22°. Fig.6c shows XRD patterns for the PA doped natural polymers display characteristic peaks as assigned to resin (R) $2\theta = 26.11^\circ, 35.73^\circ,$ and 30.25° (maximum intensity) which corresponds to the intermolecular interaction. Fig.6d shows XRD patterns for the MnPA doped natural polymers display characteristic peaks as assigned to resin ($2\theta = 26.07^\circ, 35.65^\circ$ and 30.20°). The pattern shows orthohombic structure and is in good agreement with JCPDS card number (88-2037) [20]. The (hkl) values for some of the most prominent peaks are (101), (102) and (002) which corresponds to the interplanar distance. The characteristic peak also revealed that the PA structure is preserved after incorporation with natural polymers. The crystallite size is estimated according to the Debey-Scherrer equation [21, 22].

$$D = k \lambda / \beta \cos \theta$$

Where, D is the mean grain size (nm); k the constant (shape factor, approximately (1.0)); λ represents the X-ray wavelength (0.154 nm for Mn k_{α}), β stands for the line broadening at half the maximum intensity and θ is the Bragg angle. It can be seen the average size of nanocrystals increases as doping Polyacid-Natural polymer is increased. The increasing in particle size is also clear from the decreasing in the full width at half maximum (FWHM) of the XRD Peaks. The lattice parameter calculated for the major three peaks for all the samples. The grain size and crytallinity of PA, MnPA, PA-R and MnPA-R are shown in Table 2.

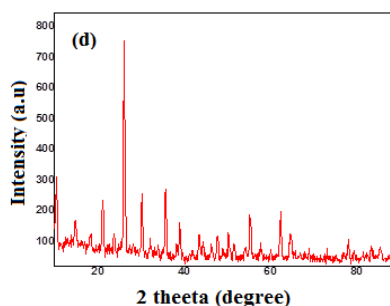
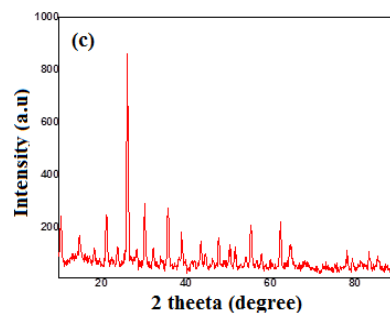
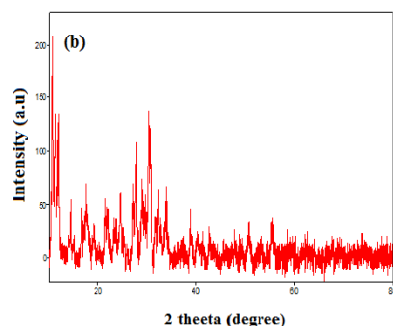
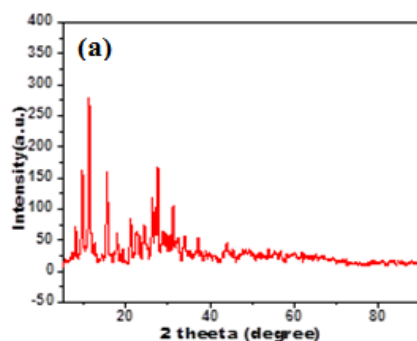


Fig.6. XRD pattern of (a) PA (b) MnPA, (c) PA-R and (d) MnPA-R

Table 2: Crystalline Grain size of PA, MnPA, PA-R, MnPA-R

S. No	Samples	2θ Values	'D'-Grain size values (nm)
1	PA	11.19	18
		15.46	20
		27.59	22
2	MnPA	28.50	26
		30.27	17
		41.22	16
3	PA-R	26.11	23
		35.73	22
		30.25	22
4	MnPA-R	26.07	19
		35.65	21
		44.21	31

3.4. Antibacterial Activity

Antibacterial activity of the compounds was tested in vitro by the well distribution method [23] against the bacteria *E. coli* and *Staphylococcus aureus*. The zone of inhibition values of the considered compounds against the bacteria are precised in Table 3. Antimicrobial experiment of PA and MnPA doped natural polymers (resin) effectively acts on Gram positive and Gram negative cell activity. Thus, the listed of Gram positive and Gram negative activity of PA and Mn-PA doped natural polymers, as shown in Fig.7 with bar chart.

In this experiment, the results have confirmed that the anti-microbial activity of natural polymers. The PA and MnPA doped (resin) natural polymer shows high Gram negative (*Escherichia coli* I and II) $\pm 18\text{mm}$; $\pm 12\text{mm}$; $\pm 13\text{mm}$ and $\pm 14\text{mm}$ (*Staphylococcus aureus* I and II)

$\pm 16\text{mm}$; $\pm 10\text{mm}$; $\pm 16.5\text{mm}$ and $\pm 16\text{mm}$ due to interaction of natural polymer over PA which corresponds to enzymatic modifications.

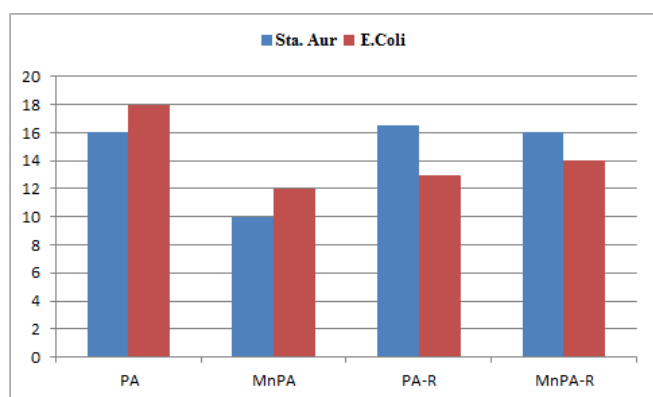


Fig.7. (Bar chart) Anti-microbial activity of PA, MnPA, PA-R and MnPA-R

Table 3: Anti-microbial activity of PA, MnPA, PA-R and MnPA-R

Compound	Zone of Inhibition (mm) (activity index) std	
	Gram (+) ve	Gram (-) ve
	<i>Staphylococcus aureus</i>	<i>Escherichia Coli</i>
PA	16mm	18mm
MnPA	10mm	12mm
PA-R	16mm	13mm
MnPA-R	16mm	14mm

4. CONCLUSION

PA and Mn-PA doped natural polymers are synthesized and characterized by using FT-IR which shows the presence of prominent peaks which explains the structure. SEM image shows that morphological structure on the PA and Mn-PA doped natural polymer (*Prosopis juliflora* resin). The XRD studies confirm the crystallite size of PA and Mn-PA doped natural polymers. The grain size is around 10 micro scales.

Acknowledgement

The financial support from the Don Bosco Research Grant, Sacred Heart College, Tirupattur is greatly appreciated.

REFERENCE

[1] Jiangwei Zhanga, Yichao Huang, Gao Lib, Yongge Weia, Recent advances in alkoxylation chemistry of polyoxometalates: From synthetic strategies, structural overviews to functional applications. *Coord. Chem. Rev.* 378(2019) 395-414.

[2] S.S.Wang, G.Y.Yang, Recent Advances in Polyoxometalate-Catalyzed Reactions. *Chem. Rev.* 115(2015) 4893-4962.

[3] Z.J. Liu, X.L. Wang, C. Qin, Z.M. Zhang, Y.G. Li, W.L. Chen, E.B. Wang, Polyoxometalate-assisted synthesis of transition-metal cubane clusters as artificial mimics of the oxygen-evolving center of photosystem. II *Coord. Chem. Rev.* 313(2016) 94-110.

[4] J.J. Walsh, A.M. Bond, R.J. Forster, T.E. Keyes, Hybrid Polyoxometalate materials for photo (electro) chemical applications. *Coord. Chem. Rev.* 306(2016) 217-234.

[5] J.W. Zhang, Y.C. Huang, Y.G. Wei, Trends in Polyoxometalates Research. Nova Sci. Publishers.(2015) 454.

[6] J.Trenton, A.Mark, Barteau, Cation exchange effects on methanol oxidation and dehydration by supported Polyoxometalates. *J. of Catalysis.* 371(2019) 357-367.

[7] M.A. Barteau, J.E. Lyons, I.K. Song, Surface chemistry and catalysis on well defined oxide surfaces: nano scale design bases for single-site heterogeneous catalysts. *J. Catal.* 216(2003) 236-245.

[8] P.Deshlahra, R.T. Carr, S.-H. Chai, E. Iglesia, Mechanistic details and reactivity descriptors in oxidation and acid catalysis of methanol. *ACS Catal.* 5(2015) 666-682.

[9] Y. F. Song, R. Tsunashima, recent advances on polyoxometalate-based molecular and composite materials. *Chem. Soc. Rev.* 41(2012) 7384-7402.

[10] A.Dolbecq, E. Dumas, C.R. Mayer, P. Mialane, Hybrid Organic-Inorganic Polyoxometalate Compounds: From Structural Diversity to Applications. *Chem. Rev.* 110(2010) 6009- 6048.

[11] Dandan Li, Pengtao Ma, Recent advances in transition-metal-containing Keggin-type polyoxometalates-based coordination polymers. *Coordination Chemistry Reviews.* 392(2019) 49-80.

[12] S.S.Wang, G.-Y. Yang, Recent Advances in Polyoxometalate-Catalyzed Reactions. *Chem. Rev.* 115(2015) 4893-4962.

[13] J.M.Clemente-Juan, E. Coronado, A. Gaita-Ariño, Magnetic polyoxometalates: from molecular magnetism to molecular spintronics and quantum computing. *Chem. Soc. Rev.* 41(2012) 7464-7478.

[14] Y.Wang and S.Sukhishvili, Hydrogen-bonded polymer complexes and nanocages of weak polyacid templated by a Pluronic block copolymer. *Soft matter.* 12(2016) 8744.

[15] Kazuyoshi Ogasawara, Multiplet Energy Level Diagrams for Cr³⁺ and Mn⁴⁺ in Oxides with Oh Site Symmetry Based on First-Principles Calculations. *J. Solid State Sci and Tech.* 5(2016) 3191-3196.

- [16] S.M.Lauinger, Polyoxometalate Multi electron Catalysts in Solar Fuel Production. 69(2017) 117-154.
- [17] Sammanan Bharath, Praveen Peter, Martin Sowriappan and Thavasikani Jeyabalan, Synthesis, characterization and anti-microbial studies of Keggin anion doped bio-polymers. Inter. J. of Recent Sci. Res. 9(2018) 23480-23485.
- [18] R.Thouvenot and M.Fournier, Vibrational Investigations of Polyoxometalate. Isomerism in Molybdenum (VI) and Tungsten (VI) compounds related to the Keggin structure. Inorg. Chem. 2(1994) 598-599.
- [19] Sammanan Bharath, Praveen Peter, Martin Sowriappan and Thavasikani Jeyabalan, Synthesis, characterization and anti-microbial studies of Keggin anion doped bio-polymers. Inter. J. of Recent Sci. Res. 9(2018) 23480-23485.
- [20] S.C. Abrahams, and JM,Reddy Crystal Structure of the Transition-Metal Molybdates and Tungstates. III. Diamagnetic α -ZnMoO₄. J. of chem. Phys. 46(2017) 2052-2061.
- [21] P.Scherrer, GottingerNachrichten Gesell. 98(1918) 2.
- [22] A.Patterson, The scherrer formula for X-Ray particle size Determination. Phys. Rev. 56(1939) 978-982.
- [23] O.N.Irobi, M.Moo-Young, and W.A.Anderson Antimicrobial Activity of Annatto (BixaOrellana) Extract. Int J Pharm. 34(1996) 87-90.